1999

Modeling the Effects of Doliolids on the Plankton Community Structure of the Southeastern US Continental Shelf

A. G. Edward Haskell
Old Dominion University

Eileen E. Hofmann
Old Dominion University, ehofmann@odu.edu

Gustav-Adolf Paffenhofer

Peter G. Verity

Original Publication Citation

Haskell, A. G. E., Hofmann, E. E., Paffenhofer, G. A., & Verity, P. G. (1999). Modeling the effects of doliolids on the plankton community structure of the southeastern US continental shelf. *Journal of Plankton Research, 21*(9), 1725-1752. doi:10.1093/plankt/21.9.1725

Journal of Plankton Research Vol.21 no.9 pp.1725–1752, 1999

Modeling the effects of doliolids on the plankton community structure of the southeastern US continental shelf

A.G.Edward Haskell, Eileen E.Hofmann, Gustav-Adolf Paffenhöfer[1] and Peter G.Verity[1]

Center for Coastal Physical Oceanography, Old Dominion University, Norfolk, VA 23529 and [1]Skidaway Institute of Oceanography, 10 Ocean Science Circle, Savannah, GA 31411, USA

Abstract. A model of the lower trophic levels that consists of a system of coupled ordinary differential equations was developed to investigate the time-dependent behavior of doliolid populations associated with upwelling features on the outer southeastern US continental shelf. Model equations describe the interactions of doliolids with two phytoplankton size fractions, five copepod developmental stages and a detrital pool. Additional equations describe nitrate and ammonia. Model dynamics are based primarily upon data obtained from field and laboratory experiments for southeastern US continental shelf plankton populations. Variations on a reference simulation, which represents average upwelling conditions without doliolids, were carried out to determine the effect of inclusion of doliolids, temperature and nutrient variations, and variations in ambient food concentrations on the basic plankton community structure. These simulations provide a measure of the role of environmental versus biological interactions in structuring the planktonic food web on the southeastern US continental shelf. Simulations show that the copepod population is significantly reduced when doliolids are present. This happens primarily as a result of direct predation of the doliolids on copepod eggs and juveniles as opposed to an increase in competition for phytoplankton, the primary food source. Additional simulations show that the cooler temperatures associated with the newly upwelled water temporarily decrease the growth rates of the doliolids and copepods, bestowing an even greater advantage on the rapidly reproducing doliolids.

Introduction

Stefánsson *et al.* (1971) first suggested that primary productivity on the outer SouthEastern US continental Shelf (SEUSS) is affected by pulses of upwelled nutrients from the waters below the Gulf Stream. Since that time, many studies have examined the physical (e.g. Yoder *et al*., 1981; McClain and Atkinson, 1985; Lee *et al*., 1991) and biological (e.g. Deibel, 1982a,b; Paffenhöfer *et al*., 1984; Verity *et al*., 1993) aspects of upwelling of this region. Now it is well known that Gulf Stream-induced upwelling provides a regular though intermittent source of nitrate and other nutrients to the outer SEUSS (e.g. Atkinson *et al*., 1978; Yoder *et al*., 1983; Paffenhöfer *et al*., 1987), through either cold-core Gulf Stream frontal eddies or bottom intrusions of Gulf Stream water (e.g. Atkinson *et al*., 1987; Lee *et al*., 1991; Verity *et al*., 1993); however, the two types of upwelling processes differ in their spatial and temporal scales. The frontal eddies occur throughout the year with a frequency of 2–14 days (Lee and Atkinson, 1983) and normally exist for only a few days (Lee *et al*., 1991), while the bottom intrusions, primarily during late winter and spring, occur every 14–40 days and may persist for up to 6 weeks (Atkinson *et al*., 1984, 1987). These episodic upwelling and intrusion events produce plankton blooms in the SEUSS waters (Atkinson *et al*., 1978; Yoder *et al*., 1981).

This study is particularly concerned with bottom intrusions in a specific portion

of the South Atlantic Bight. As the Gulf Stream flows northward past the South Carolina coast, a bathymetric rise near 32°N, known as the Charleston Bump (Figure 1), produces the Charleston Gyre, a cyclonic semi-permanent offshore meander that resides over the slope (Brooks and Bane, 1978; McClain and Atkinson, 1985). The gyre persists long enough for complex interactions to develop among phytoplankton, copepods and gelatinous zooplankton (Paffenhöfer *et al.*, 1995).

As the intruded waters age, the composition of the plankton population undergoes species succession. Within the first 3–8 days following the initial upwelling event, the small phytoplankton [<10 μm equivalent spherical diameter (ESD)] show a rapid increase. After approximately a week, the larger phytoplankton (>10 μm) become dominant. This is followed within 5–7 days by a bloom of zooplankton. The dominant copepods of the gyre are the calanoid *Paracalanus* sp. and the cyclopoid *Oithona* sp., and the vast majority of Thaliaceans, doliolid tunicates, are *Dolioletta gegenbauri* (Paffenhöfer *et al.*, 1995). The doliolids have faster growth and reproduction rates than do copepods and, therefore, at times they dominate the planktonic ecosystem of the SEUSS. This has implications for nutrient and carbon cycling of this system, and for the fate of primary production resulting from upwelling.

To examine the interactions of doliolid, copepod and phytoplankton populations on the outer SEUSS, a time-dependent numerical model was used to analyze the biological interactions of the local plankton and the changes in the community structure resulting from upwelling-induced environmental influences.

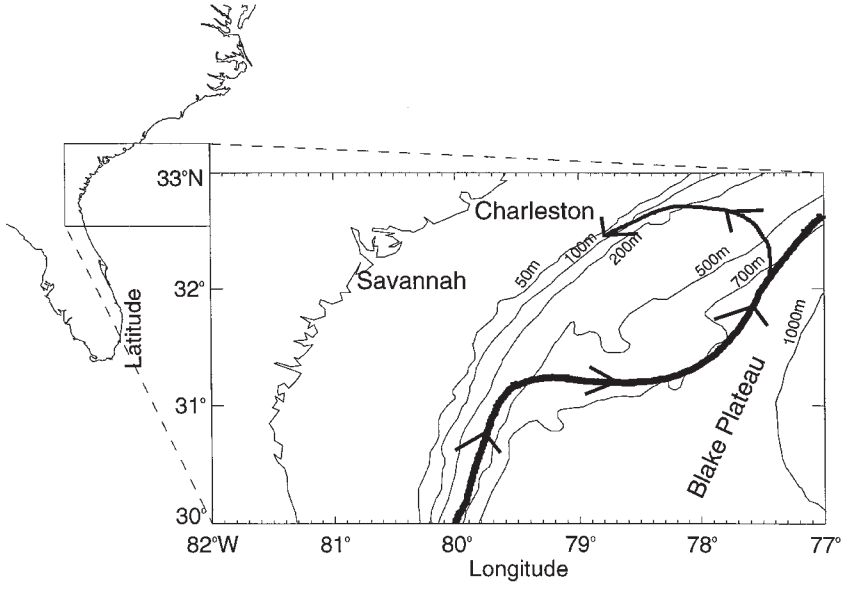

Fig. 1. Location of the study area. The thick line signifies the path of the Gulf Stream. The thinner line is the meander.

The model describes the time-dependent interactions between doliolids, two size classes of phytoplankton, five life stages of copepods, nitrate, ammonia and a detrital pool. The temperature and nitrogen content of the simulated ecosystem were varied to simulate the occurrence of Gulf Stream-induced upwelling.

This study was designed to investigate the following research questions. (i) What are the effects of temperature changes on the relative biomass density of the doliolids and the copepods? (ii) What time scale is required, following an upwelling event, for the doliolid populations to reach concentrations that produce significant effects on the density of copepod biomass? (iii) What are the concentrations needed, of all plankton fractions, for the doliolids to produce significant effects on the density of copepod biomass? (iv) Do the doliolids affect the copepods directly (by direct predation) or indirectly (by consuming a large portion of the food sources available for the copepods)? (v) How do the relative concentrations of small and large phytoplankton affect the doliolid/copepod population structure?

Method

Original model components

The time-dependent model developed for this study is a modification of the one developed by Hofmann and Ambler (1988) for the SEUSS waters. The model originally consisted of 10 ordinary differential equations representing two size classes of phytoplankton, nitrogen, ammonium, five size classes of zooplankton (the copepod *Paracalanus* sp.) and a detrital term used for closure. All model components are expressed in terms of μg N l^{-1}. The terms in the equations that were modified for the inclusion of doliolids are discussed in detail below. The Appendix lists the original equations and the definitions of the terms in the equations are given in Tables A-I through A-III, as modified for this study. Details for the original model components are found in Hofmann and Ambler (1988). A schematic of the interactions of the time-dependent model is shown in Figure 2.

The phytoplankton are grouped into one of two size classes: larger than or smaller than 10 μm [equations (A-1) and (A-2)]. Model terms for the phytoplankton include growth, cell death and zooplankton grazing. Parameterization for the processes is in equations (A-2.1)–(A-2.7).

Phytoplankton loss is modeled by a linear term that represents the fraction of the phytoplankton that is removed from the system each day. This term represents all phytoplankton losses other than through copepod and doliolid grazing, e.g. cell autolysis and sinking. Starting with an initial assumption of 0.1 day^{-1} for both phytoplankton size fractions, the value of the loss variable was adjusted to produce concentrations similar to those observed on the SEUSS.

The copepods are grouped into five classes based on development stage: egg through nauplius 2 stage (EggN2), nauplius 3 to nauplius 4 (N3N4), nauplius 5 to copepodite 3 (N5C3), copepodite 4 to copepodite 5 (C4C5), and adult (Adult). The governing equations for the different copepod stages include assimilation, excretion, egg production, molting and predation processes [equations (A-3)–(A-5)].

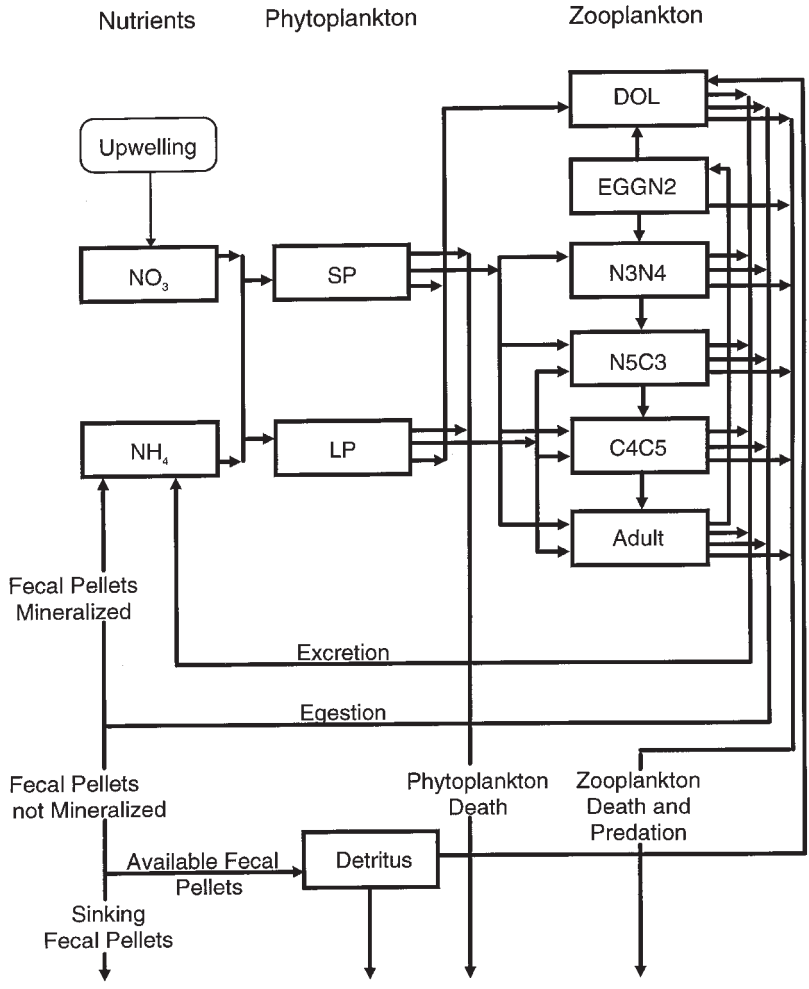

Fig. 2. Schematic of the biological components and interactions included in the model. See the text for details.

The primary source of nitrogen for the model ecosystem is nitrate. The nitrate equation [equation (A-2.2)] consists of a loss to phytoplankton via nitrogen uptake and an input term from upwelling events. The total nitrate input during a single upwelling event is divided into equal time intervals based on the duration of each event. The total amount of nitrate upwelled during a single event was specified using a linear nitrate–temperature relationship of the form suggested by Atkinson *et al.* (1984).

The other source of nitrogen in the system is ammonia. The ammonia equation [equation (A-2.3)] consists of loss to phytoplankton through ammonia uptake, and increases from excretion and remineralization of fecal pellets from both the copepods and doliolids.

The detrital component [equation (A-6)] increases as the zooplankton produce fecal pellets and decreases as the doliolids ingest the floating fecal pellets. To ensure mass conservation, a state variable was used to account for the nitrogen that would be lost by advective and other biological processes.

Model modifications

Studies, e.g. Deibel (1982b) and Crocker *et al*. (1991), have shown that the *Doliolletta* gonozooids and phorozooids feed at similar rates and can, therefore, for the purpose of this model, be treated as a single class.

Thus, the biomass density of the doliolids, D, over time (t) is determined by:

$$\frac{\mathrm{d}D}{\mathrm{d}t} = AE\left(\frac{D}{DT}P_i\right)F_{\mathrm{dol}} - \beta D \cdot aDW^b - D \cdot P_{\max}\left(1 - \mathrm{e}^{-\varepsilon(D - T_D)}\right)\cdot M(D,T_D) - \frac{D}{DT}\,N_{\max} \quad (1)$$

specifying assimilated ingestion, excretion, predation by higher trophic levels and natural mortality.

Doliolid ingestion

The doliolid, being a non-selective filter feeder, ingests particles at a rate, I, depending on the concentration of the particles and the filtration rate of the doliolid, which is expressed by the following equations:

$$I = I_{SP} \cdot J(SP,T_{SP}) + I_{LP} \cdot K(LP,T_{LP}) + I_{EggN2} + I_{Det} \quad (2)$$

where I_{SP} is the ingestion rate of the small phytoplankton size fraction given by:

$$I_{SP} = \left(\frac{D}{DT}\,SP\right)F_{\mathrm{dol}} \quad (3)$$

I_{LP} is the ingestion rate of the large phytoplankton size fraction:

$$I_{LP} = \left(\frac{D}{DT}\,LP\right)F_{\mathrm{dol}} \quad (4)$$

I_{EggN2} is the ingestion rate of the egg through nauplii 2 copepod size fraction:

$$I_{EggN2} = \left(\frac{D}{DT}\,EggN2\right)F_{\mathrm{dol}} \quad (5)$$

I_{Det} is the ingestion rate of the detrital fraction:

$$I_{Det} = \left(\frac{D}{DT}\,Det\right)F_{\mathrm{dol}} \quad (6)$$

J and K are threshold functions, DT is the weight of an average doliolid and F_{dol} is the clearance rate of the doliolids expressed as:

$$F_{dol} = F_{dol}^{max}\, e^{-0.01\, LP} \tag{7}$$

where F_{dol}^{max} is the maximum flow of water through the doliolid body cavity. The exponential term represents a decrease in flow due to clogging of the animal's filtering apparatus by the large phytoplankton class (Deibel, 1982b). The clearance rate was formulated for 20°C and then modified to allow for temperature dependence. Because there are currently no good estimates of the Q_{10} for the doliolids, a Q_{10} of 3, assuming a 'standard' poikilothermic organism, was used for this study. The clearance rate was multiplied by the factor $0.1189e^{0.107T}$, which increases and decreases the rate of clearance exponentially above and below 20°C. Values and references for the parameters used in the doliolid equations are listed in Table I.

The efficiency with which *Dolioletta* assimilates food was assumed to vary with ingestion rate, similar to the approach used by Moisan and Hofmann (1996). The assimilation efficiency AE can be expressed in terms of a maximum (AE_{max}) and minimum (AE_{min}) value as:

$$AE = AE_{min} + \left[\left(AE_{max} - AE_{min}\right) e^{-I\tau}\right] \tag{8}$$

where the e-folding scale given by τ is modified by the ingestion rate, I (Landry *et al.*, 1984). As higher food concentrations produce a higher ingestion rate, the assimilation efficiency decreases toward the minimum value. Assimilated ingestion can be calculated by multiplying the ingestion rate and the assimilation efficiency.

Doliolid excretion

The excretion rate, EX, for *Dolioletta* was obtained using a relationship suggested by Omori and Ikeda (1984), and modified by Moisan and Hofmann (1996), that relates body weight and temperature as:

$$EX = \beta D \cdot aDW^{b} \tag{9}$$

where the effect of temperature, T, is included in the coefficients that modify the doliolid dry weight, DW, and are expressed as:

$$a = 10^{0.02438T - 0.1838} \tag{10}$$

$$b = -0.01090T + 0.8918 \tag{11}$$

β is a constant equaling 1.44 [μg (μl O_2^{-1})] that includes doliolid body weight (8.33 μg N), the respiratory quotient (0.97), the molecular weight of nitrogen (14.0 μg

Table I. Units, definitions, values and sources for the parameters used in the doliolid equations

Parameter	Units	Definition	Value	Source
I	μg N l^{-1} s^{-1}	Ingestion rate	Variable	Calculated
D	μg N l^{-1}	*Dolioletta* concentration	Variable	Calculated
DT	μg N (dol^{-1})	Weight of average doliolid	8.33	Mackas *et al*., 1991
DW	μg (dol^{-1})	Total dry weight of an average doliolid	83.3	Moisan, 1993
F_{dol}^{max}	l s^{-1}	Maximum filtration rate	1.678×10^{-6}	Deibel, 1982a,b
AE_{max}	None	Maximum assimilation efficiency	0.95	Omori and Ikeda, 1984
AE_{min}	None	Minimum assimilation efficiency	0.70	Omori and Ikeda, 1984
τ	l s μg N^{-1}	Assimilation efficiency curve constant	1.466×10^{4}	Estimated this study
Γ_d	day^{-1}	Fecal pellet remineralization rate	0.10	Moisan, 1993
ρ_d	None	Fecal pellet sinking ratio	0.60	Calculated
RQ	None	Respiratory quotient	0.97	Omori and Ikeda, 1984
CN	μg C μg N^{-1}	Carbon to nitrogen ratio	3.60	Omori and Ikeda, 1984
P_{max}	μg N dol^{-1} s^{-1}	Maximum predation rate	1.736×10^{-7}	Estimated this study
ε	l μg N^{-1}	Predation rate curve constant	0.06935	Estimated this study
T_D	μg N l^{-1}	Minimum doliolid concentration for predation to occur	1.0	Moisan, 1993
N_{max}	μg N dol^{-1} s^{-1}	Maximum natural death rate	1.736×10^{-7}	Moisan, 1993

N μmol^{-1} N), doliolid dry weight (83.3 μg), liters of O_2 consumed per mole of C produced (22.4 μl O_2 μmol^{-1} C) and the C:N molar ratio (4.2).

The ingestion, assimilation and excretion of the doliolids are dependent on the effective food concentration (Figure 3).

Doliolid predation and natural mortality

Predation mortality, P, of *Dolioletta* ranges from zero below some threshold concentration, T_D, of the *Dolioletta* to a maximal predation rate, P_{max}, given by:

$$P = \frac{D}{DT} \cdot P_{max} \left(1 - e^{-\varepsilon(D - T_D)}\right) \cdot M(D,T_D) \tag{12}$$

where the threshold function, M, is expressed as follows:

$$\begin{aligned} M(D,T_D) &= 0 \text{ for } D < T_D \\ M(D,T_D) &= 1 \text{ for } D \geq T_D \end{aligned} \tag{13}$$

Natural mortality, N, of *Dolioletta* is a linear function of the doliolid concentration expressed as:

$$N = \frac{D}{DT} N_{max} \tag{14}$$

The maximum natural mortality rate, N_{max}, is chosen such that the turnover time, excluding predation pressures, is within the average *Dolioletta* lifespan of 29–41 days (Deibel, 1982a).

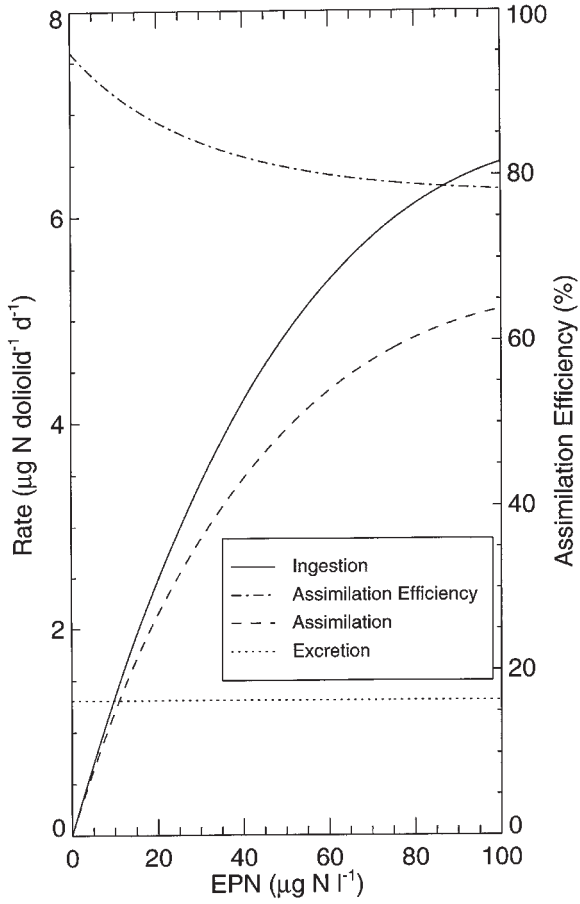

Fig. 3. Relationship between the rate of doliolid ingestion, assimilation, excretion, assimilation efficiency and effective food concentration (*EPN*) at 20°C.

Detrital components

The question of how to treat properly the detrital component of biological models still lacks a definite answer. Many studies have looked at the size, sinking rate and production rate of fecal pellets produced by different zooplankton species (e.g. Pomeroy and Deibel, 1980; Bruland and Silver, 1981; Uye and Kaname, 1994). The fate of smaller pellets has been addressed in detail by only a few studies (e.g. Paffenhöfer and Knowles, 1979; Hofmann *et al.*, 1981). Hofmann *et al.* (1981) modeled the fate of fecal pellets produced by *Paracalanus* on the SEUSS and found that the percentage of fecal pellets reaching the benthos was directly related to the size of the fecal pellet, with only 0.3, 3 and 10% of the pellets produced by the nauplii, copepodites and adults, respectively, reaching the sea floor. These percentages are used in the model as the percentage of available fecal material that is constantly removed from the system.

Estimates of the percentage of doliolid fecal material reaching the benthos of the southeastern shelf do not exist. However, Deibel (1990) estimated that doliolid fecal pellets on the SEUSS would have a residence time in the water column of 2 days or less under upwelling conditions. Using this residence time, a clearance rate of 4.4 ml zooid^{-1} h^{-1} (Deibel, 1982b; Crocker *et al*., 1991; Tebeau and Madin, 1994), and a high doliolid concentration of 2000 doliolids m^{-3}, the doliolids should only be able to ingest ~40% of the fecal pellets in the water column (ρ_d; Table I).

Along with the removal of fecal pellets via transport to the benthos, degradation of the pellets by physical and biological processes also needed to be quantified. The modeling study by Hofmann *et al*. (1981) indicated that the pellets produced by the younger copepod stages were recycled in the water column, while the adult copepod fecal pellet production accounted for most of the vertical transport. As decomposition rates of sediment trap carbon ranged from 1 to 50% day^{-1} (Iseki *et al*., 1980), values representing this range were chosen (Γ_i; in Table A-III). The fecal pellet remineralization rate for the doliolids was estimated to be similar to that used for the adult copepods because, although the doliolid fecal pellets are larger than the copepod pellets, they are less tightly compacted (Deibel, 1990; Uye and Kaname, 1994) and are more easily subjected to degradation.

Initial model analyses showed that the use of the detrital box, *DET* [equation (A-6)], to account for the nitrogen that would be lost from the model ecosystem through death, predation, advection, etc., resulted in an overabundance of doliolids. To compensate for this, a state variable was used to account for the nitrogen lost from the model ecosystem. To prevent unrealistic detrital concentrations from developing, the detrital component was flushed, at the beginning of each upwelling event with a switching function *N*:

$$\begin{aligned} N(tm,inv) &= 0 \text{ for } MOD(tm,inv) \neq 0 \\ N(tm,inv) &= 1 \text{ for } MOD(tm,inv) = 0 \end{aligned} \tag{15}$$

where *tm* is the current time step value, *inv* is the number of time steps in each upwelling event and *MOD(tm*,*inv*) is the remainder of *tm*/*inv*.

Data sets

The data sets needed for this modeling study consist of growth and ingestion rates of *Paracalanus* and *Dolioletta*, growth and nitrogen uptake data for the resident shelf phytoplankton, and nutrient and temperature data for the SEUSS ecosystem. Data for the doliolid components were taken from unpublished studies performed by G.-A.Paffenhöfer, from the Skidaway Institute of Oceanography, Savannah, GA, on the genus *Dolioletta*, and from Deibel (1982a,b) and Paffenhöfer *et al*. (1995). Copepod growth and ingestion rates were taken from Hofmann and Ambler (1988), Paffenhöfer *et al*. (1995) and from unpublished data from G.-A.Paffenhöfer. Growth and nitrogen uptake rates of the phytoplankton come from Eppley *et al*. (1969) and Yoder *et al*. (1981, 1983, 1985). Nutrient and

hydrographic data are available from many sources, e.g. Stefánsson *et al.* (1971), Atkinson *et al.* (1984) and Hofmann and Ambler (1988).

Model implementation

The solutions for the previously described system of coupled ordinary differential equations were obtained using a fourth-order Runge–Kutta numerical model with a time step of 5 min. The model was integrated forward in time until repeatable cycles were observed, which eliminated the effects of the initial conditions on the model solutions. The total nitrogen in the model (including all losses not recycled) was calculated at each time step to verify mass conservation.

Verification for all the simulation results was accomplished by comparing the model solutions to criteria obtained from field and laboratory observations of the individual biological components represented here.

The model was run forward in time with the temperature and nitrate variations repeating every 40 days, until steady cycles in the plankton structure were produced. A 40 day interval provides a sufficient period for the biological interactions to come to equilibrium and roughly approximates the duration of bottom intrusion events (Atkinson *et al.*, 1984, 1987).

The purpose of the time-dependent biological model is to investigate the effects of Gulf Stream intrusions on the biological populations of the SEUSS. Therefore, the initial values were chosen to represent actual shelf water conditions prior to these upwelling events, as discussed next.

Under conditions devoid of upwelled nutrients, the ambient nitrate concentrations in the outer SEUSS waters are usually <0.5 μM (e.g. Bishop *et al.*, 1980; Lee and Atkinson, 1983; Atkinson *et al.*, 1987). An upwelling event can increase the nitrate concentrations to a maximum of 10–15 μM within a period of 2 or 3 days (Yoder *et al.*, 1983, 1985). To simulate this nitrate input, the total nitrate supply to the model ecosystem was calculated using the nitrate–temperature relationship, discussed previously, for subsurface Gulf Stream waters along the SEUSS. The upwelling simulations described in the following section were performed using an initial temperature of 18 or 20°C with a corresponding initial nitrate concentration of ~8 or 5 μM, respectively, which was input over 2 days. Ammonium concentrations in SEUSS waters are normally <0.1 μM (Yoder *et al.*, 1983, 1985). Thus, the initial ammonium concentration for all simulations was assumed to be zero.

Both phytoplankton size fractions were initially set to 3 μg N l^{-1}, which, assuming a N:Chl *a* ratio of 6, corresponds to a chlorophyll (Chl) concentration of 1.0 μg Chl *a* l^{-1}. This value is representative of Chl concentrations found on the outer shelf during non-upwelling conditions (Yoder *et al.*, 1983, 1985). The initial concentration for the four non-adult copepod stages was set to zero and the adults were set to 0.5 μg N l^{-1}, which corresponds to nearly 500 animals m^{-3}. This is at the low end of observed copepod concentrations for the SEUSS (Paffenhöfer *et al.*, 1987, 1995). Initial doliolid concentrations were also set to either zero, for simulations without doliolids, or to low observed concentrations for the SEUSS, 0.42 μg N l^{-1}, which is approximately equal to 50 zooids m^{-3}.

Simulation results

Reference simulation

The simulations (Table II) carried out to address the primary research questions were compared to a reference simulation (Simulation 1; Table II), consisting of a constant temperature of 20°C, an initial copepod concentration equivalent to 500 copepods m^{-3}, initial equal phytoplankton size fractions totaling 1 mg Chl *a* m^{-3} and no doliolids. These values correspond to biological conditions in water in newly upwelled bottom intrusions with temperatures between 18 and 20°C (Yoder *et al*., 1983; Atkinson *et al*., 1987).

For the majority of the simulations, the temperature either remained at a constant 20°C, representing an average temperature for the outer SEUSS, or increased linearly from 18 to 25°C, representing the intrusion of cold subsurface Gulf Stream water mixing with the warmer shelf water. The relative concentrations of the two phytoplankton size fractions were adjusted by varying the phytoplankton loss rate, which determines transfers of phytoplankton to components not explicitly included in this model, e.g. to protozoa which are not included.

Specific simulations

The model was used to establish the time evolution of phytoplankton and copepod populations at a constant temperature of 20°C (Figure 4A–C). Five cycles (200 days of simulation) were needed before repeated cycles were observed in the simulated distributions. After reaching equilibrium, the time development of the simulated variables showed the succession that has been observed during outer SEUSS upwelling events. The details of the reference simulation (Table II, Simulation 1; Figure 4A–C) are described in detail in Hofmann and Ambler (1988), and are not discussed further here.

Addition of doliolids

The addition of doliolids (Simulation 2; Table II) changes the characteristics of the time evolution of the plankton populations (Figure 4D–F). Following the input of nitrate, the phytoplankton began their bloom, but the rapidly increasing

Table II. Initial conditions for the model simulations. See the text for an explanation

Simulation	Temperature (°C)	Doliolids (μg N l^{-1})	Copepods (μg N l^{-1})	LP (μg N l^{-1})	SP (μg N l^{-1})	LP loss (day^{-1})	SP loss (day^{-1})
1	20	0.00	0.50	3.0	3.0	0.07	0.14
2	20	0.42	0.50	3.0	3.0	0.07	0.14
3	20	0.42	0.50	3.0	3.0	0.04	0.11
4	20	0.42	0.50	3.0	3.0	0.11	0.17
5	20	0.00	0.50	3.0	3.0	0.04	0.11
6	18–25	0.42	0.50	3.0	3.0	0.07	0.14

All simulations were run with a nitrate input of 5 μM, except for Simulation 6 which had a nitrate input of 8 μM.

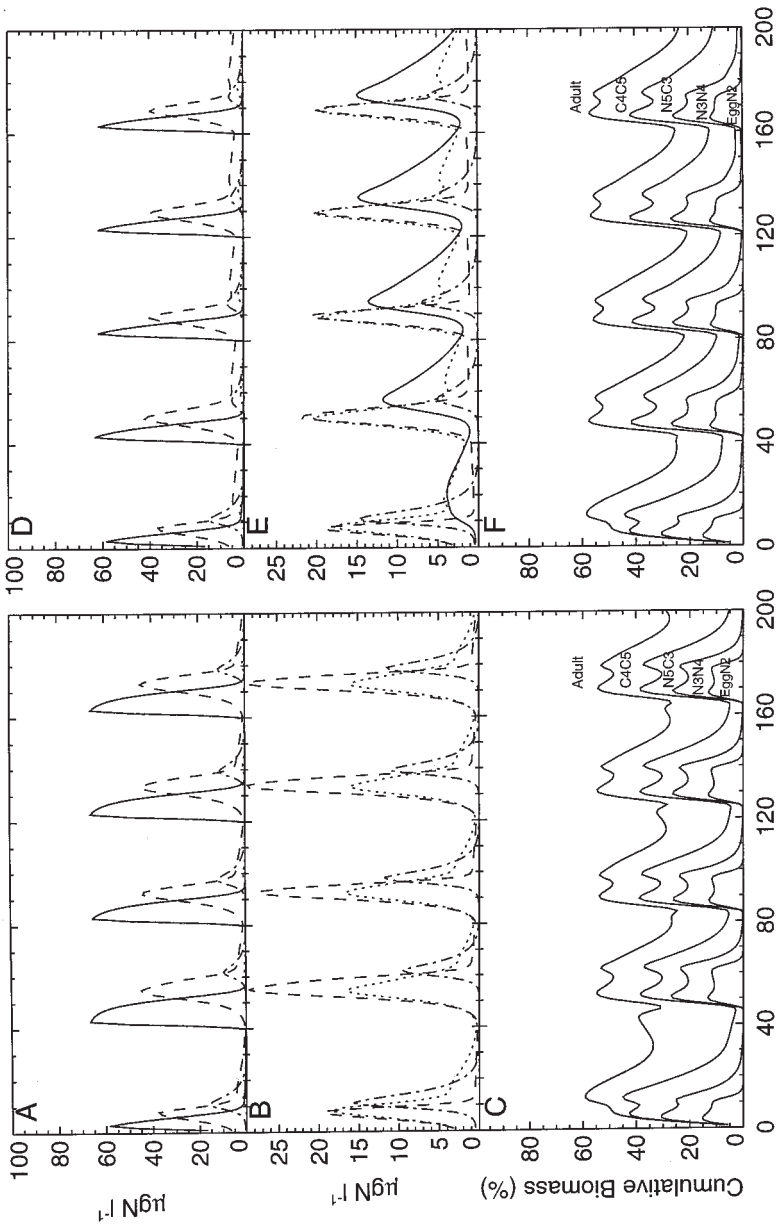

Fig. 4. Simulated time-dependent daily averaged distributions for (**A–C**) Simulation 1 and (**D–F**) Simulation 2 of Table II. (A, D) Nitrate (——), ammonium (- - - -), total phytoplankton biomass (– – –) and total copepod biomass (– - – -); (B, E) doliolid biomass (——), large phytoplankton size fraction (>10 µm) (– – –), small phytoplankton size fraction (<10 µm) (- - - -) and total copepod biomass (– - – -); (C, F) percentage of the total copepod biomass in each stage category.

number of doliolids (nearly 2000 m^{-3}) with non-selective ingestion results in about equal concentrations of small and large phytoplankton as opposed to the dominance of the large phytoplankton in the reference simulation. The doliolids did not, however, reach concentrations quickly enough to reduce significantly the overall peak phytoplankton biomass of the bloom. The duration of the simulated phytoplankton bloom was shortened from ~15 days in the reference scenario to between 8 and 9 days (Figure 4A and B versus Figure 4D and E). The presence of the doliolids inhibited the copepod production; the peak copepod biomass was reduced by 47% and the second copepod cohort was reduced in comparison to the second cohort in the reference scenario. The peak in doliolid biomass occurred a little more than 5 days later than the maximum phytoplankton concentration. Maximum simulated daily growth rates for the copepods, when doliolids were present, fell slightly to 0.60 day^{-1}, a decrease of 15%. The simulated daily growth rates for the doliolids were 0.32 day^{-1}, which falls within the 0.3–0.4 day^{-1} range that has been measured for these animals (G.-A.Paffenhöfer, unpublished).

The addition of doliolids increased the regenerated primary production, in comparison to the reference simulation, while the cumulative new production remained about the same (Table III). New production, at 54%, compared to 80% in the reference simulation, still dominated and fell near the lower end of the range observed for bottom intrusions (Yoder *et al*., 1985). The cumulative ammonium excretion by the various life stages of the copepods in the model ecosystem fell in response to the decreased numbers of copepods in the water column (Table III). The doliolids produced more ammonium than did the copepods, which accounts for the higher regenerated primary production relative to the reference case.

Biological parameters

Simulations with low loss rates (Simulation 3; Table II) and high loss rates (Simulation 4; Table II) were carried out to investigate the effect of differing relative concentrations of large and small phytoplankton on the copepod and doliolid population biomass density (Figure 5). In general, high phytoplankton loss rates produced a low biomass density of zooplankton, and vice versa. However, the important effect of the low and high loss rates is to alter the relative concentrations of the two phytoplankton size fractions (Figure 5E and H) relative to that

Table III. Production values for the phytoplankton and excretion values for the copepods calculated from the results of Simulations 1 and 2 (see Table II). All values are from the fifth 40-day cycle

	Reference	With doliolids
Phytoplankton		
Cumulative new production (μg N l^{-1})	67.0	66.9
Cumulative regenerated production (μg N l^{-1})	15.6	57.5
% regenerated production of total production	18.9	46.2
% regenerated production supported by fecal pellet remineralization	14.5	20.6
Copepods		
Cumulative NH_4 excretion (μg N l^{-1})	13.4	9.2

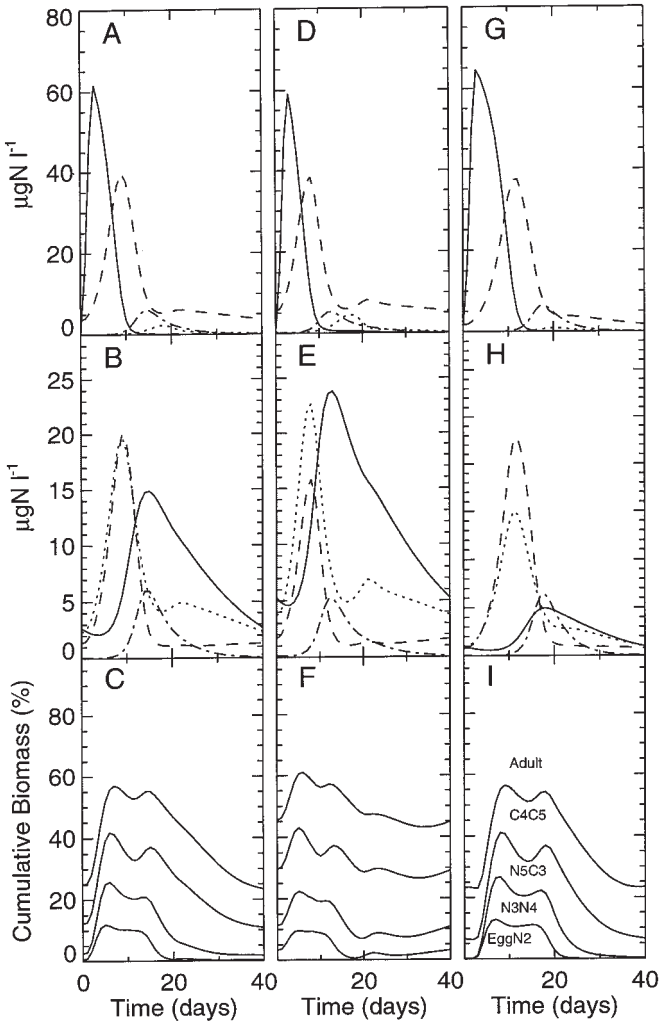

Fig. 5. Steady-state simulated distributions attained for (**A–C**) normal phytoplankton loss rates (Simulation 1); (**D–F**) low loss rate for both phytoplankton size fractions (Simulation 3); (**G–I**) high loss rates for both phytoplankton size fractions (Simulation 4). See Table II for simulation conditions. (A, D, G) Nitrate (——), ammonium (- - - -), total phytoplankton biomass (– – –) and total copepod biomass (– - – -); (B, E, H) doliolid biomass (——), large phytoplankton size fraction (>10 µm) (– – –), small phytoplankton size fraction (<10 µm) (- - - -) and total copepod biomass (– - – -); (C, F, I) percentage of the total copepod biomass in each stage category.

of those with normal loss rates (Figure 5B). The effects of the different relative phytoplankton concentrations on the zooplankton relative concentrations are described below.

Low phytoplankton loss rates resulted in simulated doliolid abundances that reached 3000 zooids m^{-3} (Figure 5E). The increased doliolids depressed the copepod growth rates due to food competition and the adult copepods were

unable to produce eggs to initiate new cohorts. The concentration of small phytoplankton allowed for maintenance of zooplankton populations, and as a result the population age structure approached equilibrium values (Figure 5F). The amount of time required for the phytoplankton to reach peak biomass was shortened to 6.8 days relative to 8.6 days in the reference simulation. High phytoplankton loss rates resulted in doliolid concentrations that did not exceed 600 m^{-3}. The doliolid concentrations are reduced because of increased competition from the copepods for the prime food source. Copepod growth rates, however, approached 0.69 day^{-1} and copepod concentrations were 20% greater than when the phytoplankton loss rates were low (Figure 5H).

To determine whether the reduction of copepods in the presence of doliolids resulted from competition for phytoplankton food or removal of copepod eggs by doliolid grazing, a simulation with low phytoplankton loss rates and no doliolids was carried out (Simulation 5; Table II). The copepod biomass is reduced relative to that in the reference simulation (Figure 6C and D versus Figure 6A and B); however, the maximum percent biomass in the EggN2 stage, the only copepod life stage that is directly preyed upon by the doliolids, was reduced by only 0.7% (Table IV). The greatest change, 8%, appeared in the N5C3 stage. Thus, reducing the simulated phytoplankton biomass reduced the copepod biomass, but did not strongly affect the percentage of copepods in each life stage. The addition of doliolids (Figure 6E and F) not only reduced the copepod biomass, but also reduced the percentage of copepods in the EggN2 stage by almost 10% (Table IV). The addition of doliolids also produced a decrease in the maximum concentration of

Table IV. Maximum percentage (%) of total copepod biomass during a 40 day upwelling cycle for the simulation without doliolids and with normal phytoplankton (Simulation 1). This value and the magnitude of the percentage change from Simulation 1 (in parentheses) is shown for simulations without doliolids and with low phytoplankton (Simulation 5) and with doliolids and normal phytoplankton (Simulation 2), respectively. Similar calculations are presented for the percentage of total copepod biomass at peak biomass

	Maximum percentage (%) of total copepod biomass during 40 day cycle		
	Simulation 1	Simulation 5	Simulation 2
EggN2	13.0	12.9 (0.7)	11.9 (8.3)
N3N4	15.0	13.9 (7.6)	14.3 (5.0)
N5C3	20.4	18.7 (8.2)	21.7 (6.4)
C4C5	24.1	26.0 (7.9)	19.8 (17.8)
Adult	73.0	72.2 (1.1)	76.6 (4.9)

	Percentage (%) of total copepod biomass at time of peak biomass		
	Simulation 1	Simulation 5	Simulation 2
EggN2	11.5	11.7 (2.0)	9.6 (16.0)
N3N4	12.2	11.1 (9.1)	11.2 (8.0)
N5C3	11.3	10.9 (3.6)	13.5 (20.0)
C4C5	17.0	17.8 (4.8)	19.6 (15.3)
Adult	48.1	48.6 (1.0)	46.1 (4.3)

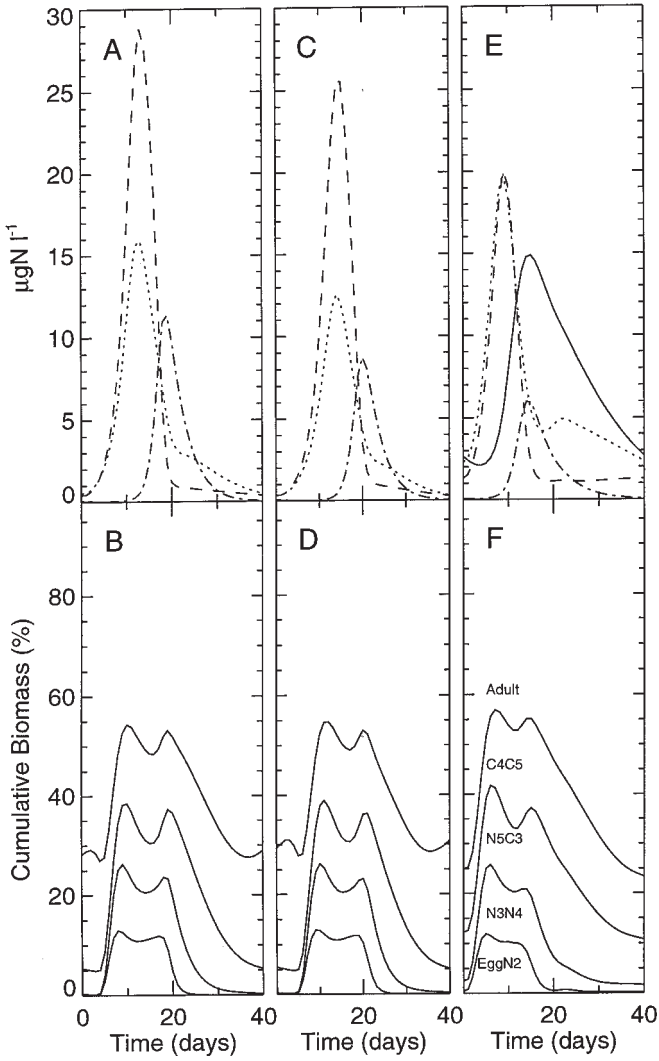

Fig. 6. Simulated time-dependent daily averaged steady-state distributions for (**A**, **B**) Simulation 1; (**C**, **D**) Simulation 5; (**E**, **F**) Simulation 2. See Table II for simulation details. (A, C, E) Doliolid biomass (——), large phytoplankton size fraction (>10 µm) (– – –), small phytoplankton size fraction (<10 µm) (- - - -) and total copepod biomass (– – – -); (B, D, F) percentage of the total copepod biomass in each stage category.

the late copepodites and adult copepods by as much as 17% (Table IV). These trends are more obvious for the population composition at peak copepod biomass.

Physical parameters

An additional simulation (Simulation 6; Table II), with a time-varying temperature profile, was carried out to examine the effects of temperature and nitrate on

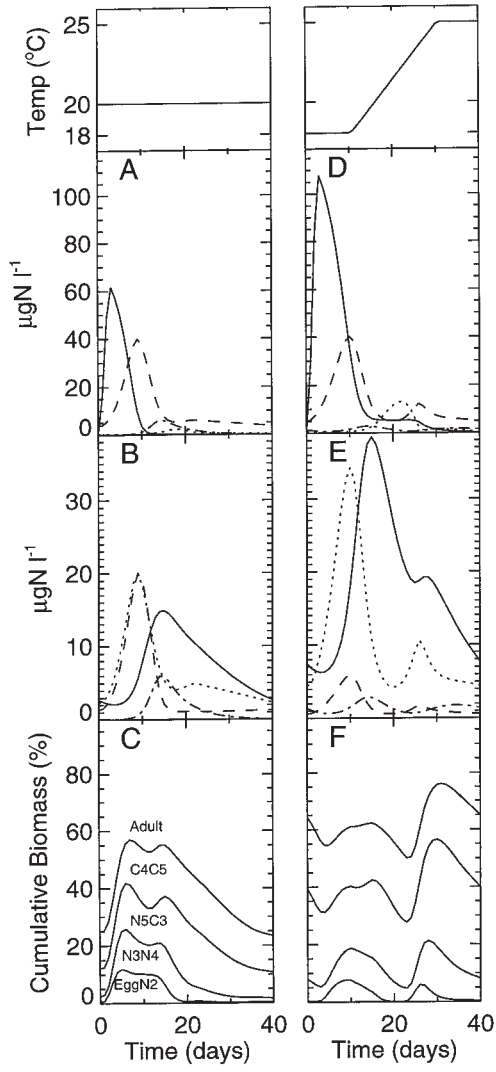

Fig. 7. Simulated steady-state solution for (**A–C**) constant temperature of 20°C, nitrate input of 5 µM over the first 2 days of the cycle (Simulation 1); (**D–F**) temperature profile shown in the top panel, nitrate input of 8 µM (Simulation 6). See Table II for simulation details. (A, D) Nitrate (——), ammonium (- - - -), total phytoplankton biomass (– – –) and total copepod biomass (– – – –); (B, E) doliolid biomass (——), large phytoplankton size fraction (>10 µm) (– – –), small phytoplankton size fraction (<10 µm) (- - - -) and total copepod biomass (– – – –); (C, F) percentage of the total copepod biomass in each stage category.

biological process in bottom intrusion waters (Figure 7D–F). In this scenario, the quantity of nitrate introduced at the beginning of each upwelling cycle has been calculated from the relationship determined by Atkinson *et al.* (1984).

Plankton growth rates, the relative biomass density of all the plankton concentrations, and the presence of the secondary peak in productivity were the prime

differences from the reference simulation. At 18°C, the metabolic rates of the plankton are reduced, with reductions in the maximum growth rates from 15%, in the small phytoplankton, to over 60% in the copepods. The 70% increase in nitrate, however, provides sufficient nutrients for the less preferred small phytoplankton size fraction to produce an intense bloom. The high doliolid concentration, >3500 animals m^{-3}, produces adequate ammonium to inhibit the phytoplankton uptake of nitrate temporarily and to initiate a secondary phytoplankton and subsequent copepod bloom.

Detrital factors

The fecal pellet remineralization rates in the reference simulation ranged from 50% day^{-1} for the small copepod nauplii fecal pellets to 10% day^{-1} for the adult copepod and doliolid pellets. To determine the effect of the remineralization rates on the simulated plankton community structure, Simulation 2 (Table II) was rerun with high and low remineralization rates. High and low rates were calculated by multiplying the initial remineralized rates (Tables A-III and I) by 1.50 and 0.50, respectively. Modifying the remineralization rates of the fecal pellets did not appear to have a notable effect on the steady-state simulated solutions (Figure 8A–C).

The same process was applied to the fecal pellet sinking rates. Simulation 2 was modified to include high and low sinking rates (Figure 8D–F). As before, high and low rates were calculated by multiplying the initial sinking rates (Tables A-III and I) by 1.50 and 0.50, respectively. The higher sinking rates considerably lowered the doliolid concentrations, while the lower sinking rates allowed the doliolid numbers to increase. The greater abundance of the doliolids, when the sinking rates were low, had a direct inverse effect on the copepod and phytoplankton populations.

Discussion

Comparison to observations

The time-dependent biological model presented in this study represents a food web in which phytoplankton production is driven chiefly by nitrate uptake rather than regenerated production from zooplankton excretion or fecal pellet remineralization. Yoder *et al*. (1985) reported new primary production values of 50–97% for bottom intrusion events in the SEUSS waters. However, during the advanced stages of a simulated bottom intrusion event, new production fell to near zero levels and there was a small increase in the <10 μm phytoplankton size fraction that was supported entirely by regenerated production (cf. Figure 4). As not all actual intrusions persist for the 40 days used in the model, many observations may not encounter these conditions.

The time-dependent biological model only included two size fractions of phytoplankton. While doliolids are not selective in their feeding behaviors, the later copepod stages exhibit a preference for the >10 μm size fraction. Because of this, it was necessary to increase the loss rate of the smaller phytoplankton

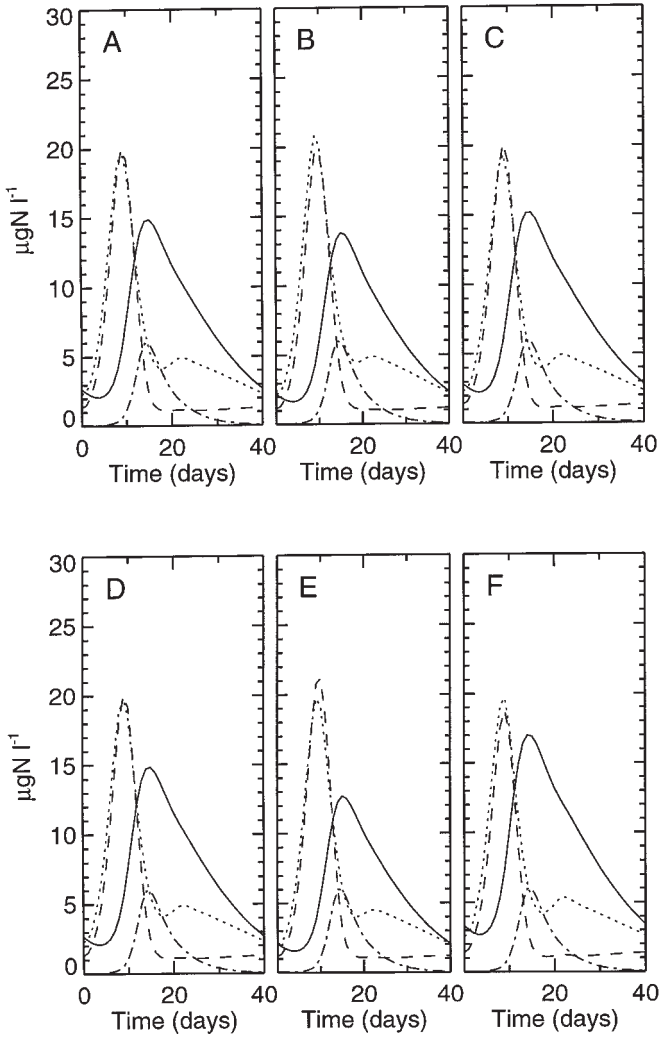

Fig. 8. Simulated steady-state time-dependent distributions of varying fecal pellet remineralization and sinking rates at 20°C for (**A**) normal remineralization rates (see Tables A-II, A-III and I); (**B**) high remineralization rates (1.5× normal); (**C**) low remineralization rates (0.5× normal); (**D**) normal sinking rates (see Tables A-II, A-III and I); (**E**) high sinking rates (1.5× normal); (**F**) low sinking rates (0.5× normal). Symbols for all panels: doliolid biomass (——), large phytoplankton size fraction (>10 µm) (– – –), small phytoplankton size fraction (<10 µm) (- - - -) and total copepod biomass (– - – -).

size fraction, relative to the large size fraction, to reproduce observed biomass densities (cf. Figure 4). This increased rate represents a loss that is currently not included explicitly in the model. The addition of protozooplankton that can graze small cells could produce the relative concentrations of the phytoplankton size fractions observed on the southeastern shelf.

In the SEUSS waters, as intrusions develop, they can become dominated by

large species of *Rhizosolenia* (>40 μm ESD), which cannot be grazed by most of the stages of *Paracalanus* (Paffenhöfer and Knowles, 1978; Paffenhöfer, 1984a,b). However, the model phytoplankton for the >10 μm size class is *Thalassiosira* (~12 μm ESD). Because of this, the model cannot adequately represent both of these larger phytoplankton and, towards the end of the intrusion, will misrepresent the large phytoplankton size fraction. The components included in the reference simulation (cf. Figure 4A–C) do, however, adequately represent the major features of Gulf Stream-induced upwelling onto the outer SEUSS.

The presence of doliolids in the outer SEUSS waters greatly alters the plankton populations observed when doliolids do not exert a strong presence (cf. Figure 4). The results of the simulations presented in this study suggest that these doliolid blooms impact the energy flow of the SEUSS ecosystem by sequestering phytoplankton biomass and converting it into tunicate biomass and fecal material.

The maximum simulated growth rates of the copepods (almost 0.70 day^{-1}) are somewhat higher than those typically observed in the field or laboratory (0.4–0.6 day^{-1}) (G.-A.Paffenhöfer, unpublished). Part of this discrepancy might be attributed to the fact that growth occurs instantaneously. Appropriate time lags from ingestion to reproduction, if present, would most likely inhibit the observed simulated growth rates as growth would be determined by the cumulative phytoplankton concentration over a given time span rather than based on instantaneous values.

Direct effects of doliolids on copepods

Paffenhöfer *et al.* (1995) found that when large doliolids were present in concentrations of 600 m^{-3} or more, the doliolids were inversely correlated with copepod concentrations in the water column. Two possible reasons for this inverse biomass relationship between copepods and doliolids are (i) the doliolid ingestion of copepod eggs and nauplii and (ii) the removal, by the doliolids, of the food source for the copepods.

During Simulation 2 (cf. Figure 4D–F), the Chl *a* concentrations do not fall below 0.5 μg l^{-1} throughout the steady-state upwelling event. At this level, *Paracalanus* should have been able to maintain its population and to reproduce at at least near half of its maximal rate (Checkley, 1980b). Thus, food concentration was most likely not severely limiting the copepod growth. Paffenhöfer *et al.* (1995) performed a gut content analyses on doliolids taken near the Charleston Gyre in January 1990, and found that almost 15% of the doliolid fecal pellets and 12% of the doliolids themselves contained one or more copepod eggs.

The simulations show that the presence of doliolids produces a larger decrease in copepod eggs than does a decrease in the food supply to the copepods (cf. Figure 6). These results imply that, while the doliolids inhibit the growth of the copepods through food competition, the direct effect of ingesting the copepod eggs has an equal if not greater effect than the reduction of the food source. Paffenhöfer *et al.* (1995) made this hypothesis based on observations from the Charleston Gyre.

Currently, there are no published numbers on doliolid ingestion rates of

copepod eggs. Experimental validation of the doliolid predation rates on the eggs and nauplii of the copepods would provide useful data for this model.

Physical processes

The temperature of the upwelled water in bottom intrusion events generally ranges from 16 to 20°C (Atkinson *et al*., 1987). These events can be identified as masses of cold subsurface water as they move onshore and alongshore. In the absence of wind mixing, the temperature of the intrusions does not change sharply over the lifetime of the event. If wind mixing does occur while the intruded waters are over the shallow shelf, then warming of the intrusion can occur as the surface water mixes with the subsurface intrusion. Since the upwelled water is on the shelf as a separate water mass, it is probable that phytoplankton develop fairly uniformly within this water. This can lead to the formation of a plankton patch in the nutrient-rich intrusion (Yoder *et al*., 1981; Atkinson *et al*., 1987).

The simulated distributions (cf. Figure 7) show that both the temperature and quantity of the introduced nutrients are important factors in determining the response of the zooplankton to the intrusions of the subsurface Gulf Stream water onto the outer SEUSS. While the cooler temperatures seen immediately following an upwelling event decrease the metabolic rates of the zooplankton, allowing the phytoplankton to utilize fully the newly input nutrients, increased grazing at the higher temperatures of the resident shelf waters directly affects the relative concentration of the two phytoplankton size fractions and thus alters the species composition of the zooplankton community. The decreased growth rates of the doliolids and copepods associated with the newly upwelled water bestow an even greater advantage to the rapidly reproducing doliolids.

Detrital factors

The formulations for the detrital factors in the ecosystem model include fecal pellet remineralization rates and fecal pellet sinking rates. As only 15–20% of the regenerated production is supported by fecal pellet remineralization, and regenerated production is only 15–20% of the total production, fecal pellet remineralization accounts for only 2–4% of the total primary production.

In contrast to fecal pellet remineralization rates, the sinking rates of the fecal pellets, and thus the rate of removal of a potential food source for the doliolids, does produce visible differences in the simulated distributions (cf. Figure 8D–F). The model is most sensitive to the sinking rates of the doliolid, in comparison to the copepod, fecal matter, as the doliolids produce >50% of all the fecal material in the water column. This occurs because doliolids ingest detritus at the same rate as phytoplankton and copepod eggs. Near the end of an upwelling cycle, fecal pellet mass, in the model system, can be >10% of the total phytoplankton biomass and can be five times greater than the total copepod biomass. Although there is currently no experimental evidence to support this, detritus could represent a significant portion of the diet of the doliolids, especially when food of high quality is available only in low concentrations.

Deibel (1990) has shown that the sinking rate of doliolid fecal pellets is strongly dependent on the doliolid diet. In order for the model to produce solutions that corresponded with observations, the doliolids were assumed to ingest 40% of the fecal material in the water column. The remaining 60% thus leaves the model ecosystem. There is the possibility that the excess fecal material could provide a significant food source to the benthic ecosystem of the outer SEUSS; however, since the outer shelf is flushed with an average periodicity of 14 days, it is possible that most of the material is advected seaward, leaving the outer shelf. Accurate production and remineralization rates of doliolid fecal pellets would increase the validity of the detrital component of ecosystem models such as the one used in this study.

Along with the removal of fecal pellets by transport to the benthos, degradation of the pellets by physical and biological processes also needs to be quantified. Recycled ammonium could possibly be a significant source of nitrogen in the late stages of a bottom intrusion. The rates at which ammonium is regenerated by bacterial decomposition of fecal pellets in the outer SEUSS waters, and their possible importance to the ecosystem, are currently not well known. The modeling study by Hofmann *et al*. (1981) indicated that the younger copepod stages produced the most fecal pellets, but that these pellets were not transported to the sea floor and were recycled in the water column. The current model simulations indicate that the fecal pellet remineralization rate does not have a large effect on the resulting plankton community structure (cf. Figure 8A–C).

Because of the high asexual fecundity and growth rates of the doliolids, each mature oozoid, i.e. a nurse with a chain, can produce literally hundreds of gonozooids in a period of several days, much shorter than the 2–4 weeks of the generation times of the other SEUSS zooplankton. The frequent flushing of the shelf with subsurface Gulf Stream water during the winter and spring can potentially maintain a temporally new community that is often dominated by the rapidly responding doliolids (Deibel, 1985). During these periods, one would expect regularly to encounter high concentrations of all the life stages of the doliolids along with a decrease in the other net zooplankton.

While a limited number of models currently include gelatinous zooplankton (e.g. Andersen and Nival, 1988; Moisan and Hofmann, 1996), the exclusion of these organisms from models of ecosystems where gelatinous zooplankton represent a significant portion of the zooplankton biomass could misrepresent the flow of matter and energy through the planktonic food webs (Hamner *et al*., 1975; Deibel, 1982a). The ability of a large (1–8 mm) zooplankter to feed directly on food as small as 2 μm represents a short trophic link in the classic food chain and could be an efficient pathway by which energy is moved from lower to higher trophic levels (Crocker *et al*., 1991). Gelatinous zooplankton are preyed upon, regularly or occasionally, by over 100 fish species; thus, they are not a trophic dead end as was previously believed (Kashkina, 1986).

The source of doliolids in the bottom intrusions remains unresolved. Deibel (1985) and Paffenhöfer *et al*. (1995) mention frequent occurrences of doliolids on the southeastern shelf during winter and spring, and possibly year round. The extremely high fecundity of the doliolids means that only a few nurses or

phorozooids are needed to start a bloom (Deibel 1985). Deibel (1985) also stated that his observations did not support the theory that the doliolids are advected into the shelf waters from the Gulf Stream, which is in contrast to the thinking of Paffenhöfer *et al*. (1995), who theorized that since Thaliacean (doliolid) occurrences are mostly episodic in nature, they do not occur continuously on the SEUSS throughout the year, and thus are most likely imported via the Florida current from the Gulf of Mexico. The response times and growth rates of the doliolids seen in the model, without a definitive source, could support either theory. Adding advective inputs to the model could help to resolve this issue.

It should be pointed out that doliolids grow from ~1 to 10 mm, with body size exhibiting a strong control on filtration and excretion rates. This model, however, simplifies the doliolid life history by representing gonozooids and phorozooids as a single size-averaged class. Smaller doliolids would not be able to ingest copepod eggs and would be able to compete with the copepods only through indirect methods. The inclusion of a juvenile doliolid class would shift some of the doliolid biomass to the small size fraction, potentially reducing the ingestion of copepod eggs and thus moving some of the biomass from the doliolids back into the copepods.

Implications and future direction

The simulation results shown in this study approximate the observed biological processes for the waters affected by the Charleston Gyre, notwithstanding that the model currently represents only a part of the SEUSS food web. While, by definition, all models provide a truncated version of the real world, additional components can be added to try to compensate for this inherent limitation. For the system considered in this study, the addition of two planktonic components, cyclopoid copepods and protozooplankton, would be desirable.

Cyclopoid copepods would provide a species with feeding and breeding habits that differ from calanoid copepods. The ability of the cyclopoid copepods to hold onto the eggs during the initial development could prevent doliolids from ingesting the same proportion as of calanoid eggs, which could result in greater concentrations of the cyclopoids.

Protozooplankton, especially ciliates, are an integral part of the SEUSS water column. The exclusion of bacteria and protozoa from the model could explain why the small phytoplankton size class needed a higher death rate than the large phytoplankton class to produce the phytoplankton composition observed in SEUSS waters. Ingestion by ciliates could equal or exceed that of doliolids. Microzooplankton, if included in the model dynamics, would most likely lower the *f*-ratio of all the scenarios and would lower the contribution of ammonium by the doliolids.

The simulations show that, when present, doliolids can reach maximum concentrations 5–7 days after the onset of an upwelling-induced phytoplankton bloom and their presence results in a rapid decrease in copepod concentrations, with the doliolids eventually displacing the copepods. This clearly suggests that the doliolids can have a major effect on nutrient and carbon cycles on the southeastern shelf and are deserving of future study, experimentally and theoretically.

Acknowledgements

This research was supported by the Commonwealth Center for Coastal Physical Oceanography at Old Dominion University and National Science Foundation grant OCE-9633401.

References

Ambler,J.W. (1986) Formulation of an ingestion function for a population of *Paracalanus* feeding on mixtures of phytoplankton. *J. Plankton Res.*, **8**, 957–972.

Andersen,V. and Nival,P. (1988) A pelagic ecosystem model simulating production and sedimentation of biogenic particles: role of salps and copepods. *Mar. Ecol. Prog. Ser.*, **44**, 37–50.

Atkinson,L.P., Paffenhöfer,G.-A. and Dunstan,W.M. (1978) The chemical and biological effect of a Gulf Stream intrusion off St. Augustine, Florida. *Bull. Mar. Sci.*, **28**, 667–679.

Atkinson,L.P., O'Malley,P.G., Yoder,J.A. and Paffenhöfer,G.-A. (1984) The effect of summertime shelf break upwelling on nutrient flux in southeastern United States continental shelf waters. *J. Mar. Res.*, **42**, 969–993.

Atkinson,L.P., Lee,T.N., Blanton,J.O. and Paffenhöfer,G.-A. (1987) Summer upwelling on the southeastern continental shelf of the U.S.A. during 1981: hydrographic observations. *Prog. Oceanogr.*, **19**, 231–266.

Bishop,S.S., Yoder,J.A. and Paffenhöfer,G.-A. (1980) Phytoplankton and nutrient variability along a cross-shelf transect off Savannah, Georgia, U.S.A. *Estuarine Coastal Mar. Sci.*, **11**, 359–368.

Brooks,D.A. and Bane,J.M. (1978) Gulf Stream deflection by a bottom feature off Charleston, South Carolina. *Science*, **20**, 1225–1226.

Bruland,K.W. and Silver,M.W. (1981) Sinking rates of fecal pellets from gelatinous zooplankton (salps, pteropods, doliolids). *Mar. Biol.*, **63**, 295–300.

Checkley,D.M.,Jr (1980a) The egg production of a marine planktonic copepod in the sea off Southern California. *Limnol. Oceanogr.*, **25**, 430–446.

Checkley,D.M.,Jr (1980b) Food limitation of egg production by a marine planktonic copepod in the sea off Southern California. *Limnol. Oceanogr.*, **25**, 991–998.

Crocker,K.M., Alldredge,A.L. and Steinberg,D.K. (1991) Feeding rates of the doliolid, *Dolioletta gegenbauri*, on diatoms and bacteria. *J. Plankton Res.*, **13**, 77–82.

Deibel,D. (1982a) Laboratory determined mortality, fecundity and growth rates of *Thalia democratica* Forskal and *Dolioletta gegenbauri* Uljanin (Tunicata, Thaliacea). *J. Plankton Res.*, **4**, 143–153.

Deibel,D. (1982b) Laboratory-measured grazing and ingestion rates of the salp, *Thalia democratica* Forskal, and the doliolid, *Dolioletta gegenbauri* Uljanin (Tunicata, Thaliacea). *J. Plankton Res.*, **4**, 189–201.

Deibel,D. (1985) Bloom of the pelagic tunicate, *Dolioletta gegenbauri*: Are they associated with Gulf Stream frontal eddies? *J. Mar. Res.*, **43**, 211–236.

Deibel,D. (1990) Still-water sinking velocity of fecal material from the pelagic tunicate *Dolioletta gegenbauri*. *Mar. Ecol. Prog. Ser.*, **62**, 55–60.

Eppley,R.W. (1972) Temperature and phytoplankton growth in the sea. *Fish Bull.*, **70**, 1063–1085.

Eppley,R.W., Rogers,J.N. and McCarthy,J.J. (1969) Half-saturation constants for uptake of nitrate and ammonium by marine phytoplankton. *Limnol. Oceanogr.*, **14**, 912–920.

Frost,B.W. (1975) A threshold feeding behavior in *Calanus pacificus. Limnol. Oceanogr.*, **20**, 263–266.

Hamner,W.M., Madin,L.P., Alldredge,A.L., Gilmer,R.W. and Hamner,P.P. (1975) Underwater observations of gelatinous zooplankton: Sampling problems, feeding biology, and behavior. *Limnol. Oceanogr.*, **20**, 907–917.

Hofmann,E.E. and Ambler,J.W. (1988) Plankton dynamics on the outer southeastern U.S. continental shelf. Part II: A time-dependent biological model. *J. Mar. Res.*, **46**, 883–917.

Hofmann,E.E., Klinck,J.M. and Paffenhöfer,G.-A. (1981) Concentrations and vertical fluxes of zooplankton fecal pellets on a continental shelf. *Mar. Biol.*, **61**, 327–335.

Iseki,K., Whitney,F. and Wong,C.S. (1980) Biochemical changes of sedimented matter in sediment trap in shallow coastal waters. *Bull. Plankton Soc. Jpn*, **27**, 27–36.

Kashkina,A.A. (1986) Feeding of fishes on salps (Tunicata, Thaliacea). *J. Ichthyol.*, **26**, 57–64.

Landry,M.R. (1983) The development of marine calanoid copepods with comment on the isochromal rule. *Limnol. Oceanogr.*, **28**, 614–624.

Landry,M.R., Hassett,R.P., Fagerness,V., Downs,J. and Lorenzen,C.J. (1984) Effect of food acclimation on assimilation efficiency of *Calanus pacificus*. *Limnol. Oceanogr.*, **29**, 361–364.

Lee,T.N. and Atkinson,L.P. (1983) Low-frequency current and temperature variability from Gulf Stream frontal eddies and atmospheric forcing along the southeast U.S. outer continental shelf. *J. Geophys. Res.*, **88**, 4541–4567.

Lee,T.N., Yoder,J.A. and Atkinson,L.P. (1991) Gulf stream frontal eddy influence on productivity of the southeast U.S. continental shelf. *J. Geophys. Res.*, **96**, 22191–22205.

Mackas,D.L., Washburn,L. and Smith,S.L. (1991) Zooplankton community patterns associated with a California current cold filament. *J. Geophys. Res.*, **96**, 14781–14797.

McClain,C.R. and Atkinson,L.P. (1985) A note on the Charleston Gyre. *J. Geophys. Res.*, **90**, 11857–11861.

Moisan,J.R. (1993) Modeling nutrient and plankton processes in the California coastal transition zone. PhD Dissertation, Old Dominion University, Norfolk, VA, 214 pp.

Moisan,J.R. and Hofmann,E.E. (1996) Modeling nutrient and plankton processes in the California coastal transition zone 1. A time- and depth-dependent model. *J. Geophys. Res.*, **101**, 22647–22676.

Omori,M. and Ikeda,T. (1984) *Methods in Marine Zooplankton Ecology.* John Wiley & Sons, New York.

Paffenhöfer,G.-A. (1984a) Does Paracalanus feed with a leaky sieve? *Limnol. Oceanogr.*, **29**, 155–160.

Paffenhöfer,G.-A. (1984b) Food ingestion by the marine planktonic copepod *Paracalanus* in relation to abundance and size distribution of food. *Mar. Biol.*, **80**, 323–333.

Paffenhöfer,G.-A. and Gardner,W.S. (1984) Ammonium release by juveniles and adult females of the subtropical marine copepod *Eucalanus pileatus*. *J. Plankton Res*., **6**, 505–513.

Paffenhöfer,G.-A. and Knowles,S.C. (1978) Feeding of marine planktonic copepods on mixed phytoplankton. *Mar. Biol.*, **48**, 143–152.

Paffenhöfer,G.-A. and Knowles,S.C. (1979) Ecological implications of fecal pellet size, production and consumption by copepods. *J. Mar. Res.*, **37**, 35–49.

Paffenhöfer,G.-A., Wester,B.T. and Nicholas,W.D. (1984) Zooplankton abundance in relation to state and type of intrusions onto the southeastern United States shelf during summer. *J. Mar. Res.*, **42**, 995–1017.

Paffenhöfer,G.-A., Atkinson,L.P., Blanton,J.O., Lee,T.N., Pomeroy,L.R. and Yoder,J.A. (1987) Summer upwelling on the southeastern continental shelf of the U.S.A. during 1981. Summary and conclusions. *Prog. Oceanogr.*, **19**, 437–441.

Paffenhöfer,G.-A., Atkinson,L.P., Lee,T.N., Verity,P.G. and Bulluck,L.R.III (1995) Distribution and abundance of thaliaceans and copepods off the southeastern U.S.A. during winter. *Cont. Shelf Res.*, **15**, 255–280.

Pomeroy,L.R. and Deibel,D. (1980) Aggregation of organic matter by pelagic tunicates. *Limnol. Oceanogr.*, **25**, 643–652.

Stefánsson,U., Atkinson,L.P. and Bumpus,D.F. (1971) Hydrographic properties and circulation of the North Carolina shelf and slope waters. *Deep-Sea Res.*, **118**, 383–420.

Tebeau,C.M. and Madin,L.P. (1994) Grazing rates for three life history states of the doliolid *Dolioletta gegenbauri* Uljanin (Tunicata, Thaliacea). *J. Plankton Res.*, **16**, 1075–1081.

Uye,S. and Kaname,K. (1994) Relations between fecal pellet volume and body size for major zooplankters of the inland Sea of Japan. *J. Oceanogr.*, **50**, 43–49.

Vanderploeg,H.A., Scavia,A.D. and Liebig,J.R. (1984) Feeding rate of *Diaptomus sicilis* and its relation to selectivity and effective food concentration of algal mixtures in Lake Michigan. *J. Plankton Res.*, **6**, 919–941.

Verity,P.G., Yoder,J.A., Bishop,S.S., Nelson,J.R., Craven,D.B., Blanton,J.O., Robertson,C.Y. and Tronzo,C.R. (1993) Composition, productivity and nutrient chemistry of a coastal ocean planktonic food web. *Cont. Shelf Res.*, **13**, 741–776.

Yoder,J.A., Atkinson,L.P., Lee,T.N., Kim,H.H. and McClain,C.R. (1981) Role of Gulf Stream frontal eddies in forming phytoplankton patches on the outer southeastern shelf. *Limnol. Oceanogr.*, **26**, 1103–1110.

Yoder,J.A., Atkinson,L.P., Bishop,S.S., Hofmann,E.E. and Lee,T.N. (1983) Effect of upwelling on phytoplankton productivity of the outer southeastern United States continental shelf. *Cont. Shelf Res.*, **1**, 385–404.

Yoder,J.A., Atkinson,L.P., Bishop,S.S., Blanton,J.O., Lee,T.N. and Pietrafesa,L.J. (1985) Phytoplankton dynamics within Gulf Stream intrusions on the southeastern United States continental shelf during summer 1981. *Cont. Shelf Res.*, **4**, 611–635.

Received on August 19, 1998; accepted on May 12, 1999

Appendix: Model equations and parameters as given in Hofmann and Ambler (1988). Modifications for doliolids are enclosed in braces, i.e. {}

$$\frac{dLP}{dt} = \frac{P_m I}{I_k + I}\frac{Chl}{C}\left[\frac{NO_3}{k_n + NO_3}\,\sigma + \frac{NH_4}{k_a + NH_4}\right] LP - \delta_{LP} LP - \sum_{i=3}^{5} \frac{W_{i,1} LP}{EPN_i}\, I_{mi}\left(1 - e^{-\gamma_i EPN_i}\right) ZN_i \left\{ - \frac{D}{DT}\, LP \cdot F_{dol} \cdot K\left(LP, T_{LP}\right)\right\} \tag{A-1}$$

$$\frac{dSP}{dt} = \frac{P_m I}{I_k + I}\frac{Chl}{C}\left[\frac{NO_3}{k_n + NO_3}\,\sigma + \frac{NH_4}{k_a + NH_4}\right] SP - \delta_{SP} SP - \sum_{i=2}^{5} \frac{W_{i,2} SP}{EPN_i}\, I_{mi}\left(1 - e^{-\gamma_i EPN_i}\right) ZN_i \left\{ - \frac{D}{DT}\, SP \cdot F_{dol} \cdot J\left(SP, T_{SP}\right)\right\} \tag{A-2}$$

$$P_m = \left(2^{\mu} - 1\right)\frac{C}{Chl} \tag{A-2.1}$$

$$\mu = 1.850(1.048)^T \tag{A-2.1.1}$$

$$\frac{dNO_3}{dt} = -\sum_{j=1}^{2}\left[\frac{P_m I}{I_k + I}\,\frac{Chl}{C}\,\frac{NO_3}{k_n + NO_3}\,\sigma\right] P_j + \begin{cases} S_0/L & \text{during upwelling events} \\ 0 & \text{during all other times} \end{cases} \tag{A-2.2}$$

$$I(t) = I_0 \begin{cases} \sin\left(\dfrac{t-6}{24}\right)\pi & \text{for } 6 < t < 18 \\ 0 & \text{for } t < 6 \text{ or } t > 18 \end{cases} \tag{A-2.2.1}$$

$$NO_3\left(\mu g\ l^{-1}\right) = 14.01(38.21 - 1.67T) \tag{A-2.2.2}$$

$$\sigma = e^{-\beta NH_4} \tag{A-2.2.3}$$

$$\frac{dNH_4}{dt} = -\sum_{j=1}^{2}\left[\frac{P_m I}{I_k + I}\,\frac{Chl}{C}\,\frac{NH_4}{k_a + NH_4}\right] P_j + \sum_{i=2}^{5}\left(\eta_i + \nu_i\, EPN_i\right) ZN_i + \sum_{i=2}^{5}\Gamma_i\left(1 - \psi_i\right)\left(1 - \rho_i\right) I_{mi}\left(1 - e^{-\gamma_i EPN_i}\right) ZN_i \left\{ + \beta D \cdot aDW^b + \Gamma_d\left(1 - AE\right)\left(1 - \rho d\right) D\right\} \tag{A-2.3}$$

$$EPN_i = W_{i,SP} SP + W_{i,LP} LP \cdot H\left(LP, T_{COP,i}\right) \tag{A-2.4}$$

$$\begin{aligned} H\left(LP, T_{COP}\right) &= 0 \quad \text{for } LP < T_{COP} \\ H\left(LP, T_{COP}\right) &= 1 \quad \text{for } LP \geq T_{COP} \end{aligned} \tag{A-2.5}$$

$$\begin{aligned} J\left(SP, T_{SP}\right) &= 0 \quad \text{for } SP < T_{SP} \\ J\left(SP, T_{SP}\right) &= 1 \quad \text{for } SP \geq T_{SP} \end{aligned} \tag{A-2.6}$$

$$\begin{aligned} K\left(LP, T_{LP}\right) &= 0 \quad \text{for } LP < T_{LP} \\ K\left(LP, T_{LP}\right) &= 1 \quad \text{for } LP \geq T_{LP} \end{aligned} \tag{A-2.7}$$

$$\frac{dZN_1}{dt} = \phi E_m\left(1 - e^{-\lambda(I_5 - E_0)}\right)ZN_5 - D_{m1,2}ZN_1 - \left(\frac{M_pZN_1}{k_1 + ZN_1}\right)ZN_1\left\{-\frac{D}{DT}ZN_1 \cdot F_{dol}\right\} \quad \text{(A-3)}$$

$$\frac{dZN_i}{dt} = \psi_i I_{mi}\left(1 - e^{-\gamma_i EPN_i}\right)ZN_i - (\eta_i + \nu_i EPN_i)ZN_i + D_{mi-1,i}\left(1 - e^{-\Lambda_{i-1}EPN_{i-1}}\right)ZN_i - D_{mi,i+1}\left(1 - e^{-\Lambda_i EPN_i}\right)ZN_i - \left(\frac{M_pZN_i}{k_i + ZN_i}\right)ZN_i \quad \text{(A-4)}$$

$$\frac{dZN_5}{dt} = \psi_5 I_{m5}\left(1 - e^{-\gamma_5 EPN_5}\right)ZN_5 - (\eta_5 + \nu_5 EPN_5)ZN_5 - \phi E_m\left(1 - e^{-\lambda(I_5 - E_0)}\right)ZN_5 + D_{m4,5}\left(1 - e^{-\Lambda_4 EPN_4}\right)ZN_5 - \left(\frac{M_pZN_5}{k_5 + ZN_5}\right)ZN_5 \quad \text{(A-5)}$$

$$D_i(T) = 1/[432DR_i(T + 2.97)^{-2.25}] \text{ for } i = 1, 2, 3, 4 \quad \text{(A-5.1)}$$

$$\frac{dDET}{dt} = \sum_{i=2}^{5}\left(1 - \Gamma_i\right)\left(1 - \psi_i\right)\rho_i\left(1 - e^{-\gamma_i EPN_i}\right)ZN_i + \left\{+\left(1 - \Gamma_d\right)\rho_d\left(1 - AE\right)I - DET \cdot N\left(tm,inv\right)\right\} \quad \text{(A-6)}$$

Table A-I. Units, definitions, values and sources for the parameters used in the phytoplankton and nutrient equations for bottom intrusions and frontal eddies (frontal eddy values, where different, are given in parentheses)

Parameter	Units	Definition	Value	Source
LP	µg N l^{-1}	Concentration of large phytoplankton size class	Variable	Calculated
SP	µg N l^{-1}	Concentration of small phytoplankton size class	Variable	Calculated
P_m	mg C mg^{-1} Chl a h^{-1}	Maximum assimilation number	Variable	Eppley, 1972
I	E m^{-2} h^{-1}	Light intensity	Variable	Calculated
I_0	E m^{-2} h^{-1}	Maximum light intensity	4.0	Yoder *et al*., 1983, 1985
I_k	E m^{-2} h^{-1}	Light intensity half-saturation constant	1.11 (1.98)	Yoder *et al*., 1983
Chl C^{-1}	mg Chl a mg^{-1} C	Chlorophyll a:carbon ratio	0.025	Yoder *et al*., 1983
NO_3	µg N l^{-1}	Nitrate concentration	Variable	Calculated
NH_4	µg N l^{-1}	Ammonium concentration	Variable	Calculated
k_n	µg N	NO_3 concentration at half-maximum uptake rate	21.7 (0.0)	Hofmann and Ambler, 1988
k_a	µg N	NH_4 concentration at half-maximum uptake rate	0.658 (0.0)	Hofmann and Ambler, 1988
σ	None	NH_4 inhibition of NO_3 uptake	Variable	Calculated
δ_{SP}	day^{-1}	Natural death rate of the small phytoplankton size fraction	0.138	Estimated this study
δ_{LP}	day^{-1}	Natural death rate of the large phytoplankton size fraction	0.068	Estimated this study
T_{COP}	µg N l^{-1}	Copepod feeding threshold on the large phytoplankton fraction	See Table A-III	Frost, 1975
T_{LP}	µg N l^{-1}	Doliolid feeding threshold on both phytoplankton fractions	0.12	Estimated this study

Table A-II. Units, definitions, values and sources for the parameters used in the copepod equations

Parameter	Units	Definition	Value	Source
ZN_i	µg N l^{-1}	Concentration of size fraction	Variable	Calculated
ϕ	None	Sex ratio (fraction of females)	0.85	Checkley, 1980a
E_m	day^{-1}	Maximum egg production	0.5	Landry, 1983
λ	day^{-1}	Egg production rate constant	1.848	Landry, 1983
W_i	None	Selectivity coefficient	See Table A-III	Ambler, 1986
$D_{mi,j}$	day^{-1}	Maximum development rate	See Table A-III	G.-A.Paffenhöfer, unpublished
DR	None	Ratio of minimum development time:egg development time @ 20°C	See Table A-III	Checkley, 1980b
Λ	l µg N^{-1}	Development rate constant	See Table A-III	G.-A.Paffenhöfer, unpublished
ψ	None	Assimilation efficiency	Variable	Calculated
I_{mi}	day^{-1}	Maximum ingestion rate	See Table A-III	Vanderploeg *et al*., 1984
η	day^{-1}	Excretion rate constant	See Table A-III	Paffenhöfer and Gardner, 1984
ν	µg N^{-1}	Excretion rate constant	See Table A-III	Paffenhöfer and Gardner, 1984
γ	l µg N^{-1}	Ingestion rate curve constant	See Table A-III	Vanderploeg *et al*., 1984
M_p	µg N l^{-1}	Maximum predation rate	Variable	Hofmann and Ambler, 1988
Γ_i	day^{-1}	Fecal pellet remineralization rate	See Table A-III	Hofmann and Ambler, 1988
k_i	µg N l^{-1}	Half-maximum predation rate	0.005	Hofmann and Ambler, 1988
BW	µg N	Body weight	See Table A-III	Paffenhöfer, 1984b
ρ_i	None	Fecal pellet sinking ratio	See Table A-III	Hofmann and Ambler, 1988

Table A-III. Values for the parameters used in the copepod equations where different values are needed for different copepod size fractions. Units and sources are listed in either Table A-I or A-II

Parameter	ZN_2	ZN_3	ZN_4	ZN_5
W_{SP}	1.0	0.33	0.103	0.085
W_{LP}	0.0	1.0	1.0	1.0
D_m	0.321	0.193	0.365	–
DR	8.32	13.85	7.35	
Λ	1.119	1.102	1.118	–
I_m	1.096	1.326	1.702	1.872
η	0.3942	0.2613	0.1134	0.1339
ν	0.0062	0.0034	0.0010	0.0005
γ	0.236	0.160	0.096	0.080
Γ_i	0.5	0.4	0.2	0.1
T_{COP}	–	0.051	0.404	0.880
BW	0.0104	0.0509	0.403	0.880
ρ_i	0.003	0.03	0.10	0.10